Renewable and Sustainable Energy Reviews 166 (2022) 112670

Contents lists available at ScienceDirect

Renewable and Sustainable Energy Reviews

journal homepage: www.elsevier.com/locate/rser

Assuring the integrity of offshore carbon dioxide storage

D.P. Connelly [a,*], J.M. Bull [b], A. Flohr [a,b], A. Schaap [a], D. Koopmans [c], J.C. Blackford [d], P.R. White [e], R.H. James [b], C. Pearce [a], A. Lichtschlag [a], E.P. Achterberg [f], D. de Beer [g], B. Roche [b], J. Li [b], K. Saw [b], G. Alendal [h], H. Avlesen [i], R. Brown [a], S.M. Borisov [j], C. Böttner [f], P.W. Cazenave [d], B. Chen [k], A.W. Dale [f], M. Dean [l], M. Dewar [d], M. Esposito [f], J. Gros [f], R. Hanz [a], M. Haeckel [f], B. Hosking [a], V. Huvenne [a], J. Karstens [f], T. Le Bas [a], T.G. Leighton [e], P. Linke [f], S. Loucaides [a], J.M. Matter [b], S. Monk [a], M.C. Mowlem [a], A. Oleynik [h], A.M. Omar [i], K. Peel [a], G. Provenzano [b,m], U. Saleem [k], M. Schmidt [f], B. Schramm [f], S. Sommer [f], J. Strong [a], I. Falcon Suarez [a], B. Ungerboeck [j,n], S. Widdicombe [d], H. Wright [a], E. Yakushev [o]

[a] National Oceanography Cene Southampton, Southampton, SO14 3ZH, UK
[b] University of Southampton Waterfront Campus, Southampton, SO14 3ZH, UK
[c] Max Planck Institute for Marine Microbiology, Celsiusstr. 1, 28359, Bremen, Germany
[d] Plymouth Marine Laboratory, Prospect Place, Plymouth, PL13DH, UK
[e] ISVR, University of Southampton, Southampton, SO17 1BJ, UK
[f] GEOMAR Helmholtz Centre for Ocean Research Kiel, Wischhofstr. 1-2, 24148, Kiel, Germany
[g] Max Planck Institute for Marine Microbiology, Bremen, Germany
[h] University of Bergen, Department of Mathematics, Realfagbygget, Allegt. 41, 5020, Bergen, Norway
[i] NORCE Norwegian Research Centre, Bjerknes Centre for Climate Research, Bergen, Norway
[j] Graz University of Technology, Rechbauerstrasse 12, 8010, Graz, Austria
[k] Heriot-Watt University, Edinburgh, EH14 4AS, UK
[l] Shell Global Solutions International B.V., Grasweg 31, 1031 HW, Amsterdam, Netherlands
[m] University Grenoble Alpes, ISTerre, Grenoble, France
[n] Pyroscience GmbH, Hubertusstr. 35, 52064, Aachen, Germany
[o] Norwegian Institute for Water Research, 5006, Bergen, Norway

ARTICLE INFO

Keywords:
CCS
Detection
Quantification
Attribution
North sea
Marine

ABSTRACT

Carbon capture and storage is a key mitigation strategy proposed for keeping the global temperature rise below 1.5 °C. Offshore storage can provide up to 13% of the global CO_2 reduction required to achieve the Intergovernmental Panel on Climate Change goals. The public must be assured that potential leakages from storage reservoirs can be detected and that therefore the CO_2 is safely contained. We conducted a controlled release of 675 kg CO_2 within sediments at 120 m water depth, to simulate a leak and test novel detection, quantification and attribution approaches. We show that even at a very low release rate (6 kg day^{-1}), CO_2 can be detected within sediments and in the water column. Alongside detection we show the fluxes of both dissolved and gaseous CO_2 can be quantified. The CO_2 source was verified using natural and added tracers. The experiment demonstrates that existing technologies and techniques can detect, attribute and quantify any escape of CO_2 from subseabed reservoirs as required for public assurance, regulatory oversight and emissions trading schemes.

1. Introduction

Capturing and storing CO_2 (CCS) is an accepted strategy for mitigating climate change [1] by removing the CO_2 from the atmosphere and reducing global warming. Storage of CO_2 has been demonstrated both onshore and offshore in aquifers or depleted hydrocarbon reservoirs. Offshore storage provides the largest and probably most cost-effective means of developing >100 GT storage by 2050 [2]. To date, particularly in the USA, enhanced oil recovery is commonly used for onshore storage, although the storage is not long term as the CO_2 is recycled for further use. Recently the U.S. Department of Energy has

* Corresponding author.
E-mail address: dpc@noc.ac.uk (D.P. Connelly).

https://doi.org/10.1016/j.rser.2022.112670
Received 6 May 2021; Received in revised form 4 May 2022; Accepted 2 June 2022
Available online 10 June 2022

List of abbreviations

CCS – Carbon Capture and Storage
MMV – Measurement, Monitoring and Verification
IPCC – Intergovernmental Panel for Climate Change
ROV – Remotely Operated Vehicle
AUV – Autonomous Underwater Vehicle
ISFET Ion Sensitive Field Effect Transistor
DIC – Dissolved inorganic carbon
ORP Oxidation-reduction potential
VPDB Vienna Pee Dee Belemnite
STEMM-CCS – Strategies for the environmental monitoring of marine CCS

identified the Gulf of Mexico as a region for long term offshore CO_2 storage [3] and is investing in exploring this potential. Most other countries with CCS ambitions are using offshore storage reservoirs: Japan has an offshore demonstration CCS project at Tomakomi, Australia has recently passed a bill that allows large scale offshore carbon dioxide storage, and in Europe most operating, and planned, storage facilities are offshore (e.g., Snøhvit, Sleipner). The main barriers for the wider use of CCS are political, public acceptance and the perceived cost of initial and ongoing operations. To promote investment in CCS, Europe has an incentivising regime, the European Union (EU) Emissions Trading Scheme (ETS), that rewards companies for permanently storing CO_2. The United States of America have recently introduced carbon capture tax credits (45Q) of up to $50 per ton of CO_2 stored permanently [4]. A secondary issue is the long-term liability for secure CO_2 storage over the whole project lifecycle, including after injection operations have ceased.

Safe, long-term containment of geologically stored CO_2 both onshore or offshore is ensured with risk-based Measurement, Monitoring and Verification (MMV) programmes public reassurance and compliance with legislation [5]. Monitoring of offshore CO_2 injection wells and changes in the subsurface reservoir follow well developed standard industry approaches. However, monitoring of offshore storage reservoirs requires novel methodologies to detect, attribute and quantify leakage defined as CO_2 seeping into the water column [4]. Robust monitoring is required for public assurance and for qualification for tax credits under the EU ETS [6]. The consensus is that the risk of storage failure is considered very small [1] but these risks must be considered in a regulatory sense. Large scale breaches of containment will potentially have more impact but would be relatively easy to detect due to loss of pressure at the injection point. However, detecting a small leak within a large area of the seabed, with often poorly understood 'normal' conditions, makes monitoring a challenge, and quantification of fugitive emissions remains difficult [7].

Attribution of CO_2 must be done to avoid 'false positives'. Natural sources of CO_2 in marine systems (e.g., biological respiration of organic material) cause variations in seawater inorganic carbon concentrations, increasing CO_2 and decreasing pH in the water column. A variance above a calculated threshold around a CCS demonstration project in Japan halted operations because it was assumed the reservoir integrity was breached. A subsequent investigation showed the CO_2 came from the microbial degradation of organic matter from a surface water phytoplankton bloom (Jun Kita, METI pers comm.). The identification of low error, high sensitivity anomaly criteria is therefore paramount.

A range of computational approaches are able to quantify impact from leakage and suggest cost-effective strategies for monitoring. These models combine benthic, hydrodynamic, and biogeochemical processes to describe the evolution of multiphase CO_2 plumes in the environment [8,9]. From these models one can derive highly sensitive low error criteria that distinguish anomalous CO_2 from natural variability, based

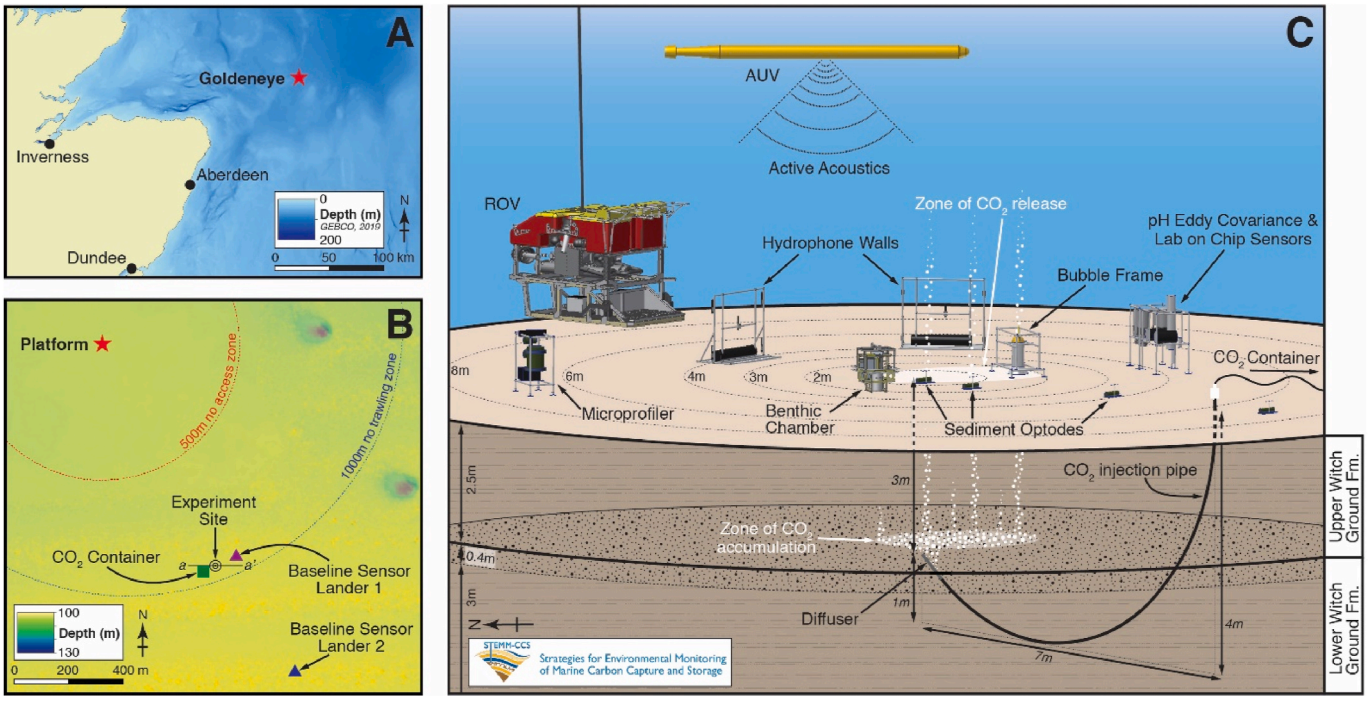

Fig. 1. Location and experimental geometry of the controlled CO_2 release experiment in the North Sea at 120 m water depth. A, Regional map showing the location of the Goldeneye Platform (red star), ~130 km NE of Aberdeen. **B**, Location of the controlled release experiment site SE of the Goldeneye Platform, seabed CO_2 container (~80 m SW of the experiment site), Baseline Sensor Landers. Chirp sub-bottom profile transect (a-a'; Fig. 3). **C**, Detailed experimental geometry around the locus of the release showing seabed instrumentation deployed by a Remotely Operated Vehicle (ROV). The CO_2 release was 3 m below the sediment surface immediately below a 30–50 cm thick sandy layer (stippling) at the top of the Lower Witch Ground formation. The rest of the Lower Witch Ground formation (~3 m) and the overlying Upper Witch Ground formation (~2.5 m) comprise moderately sorted sandy and silty muds.

on monitoring rates of change [10] and by defining stoichiometrically constrained multivariate bounds on CO_2 concentrations [11]. Simulated CO_2 release scenarios can then be used to guide optimal placement of sensors [12] and routing of autonomous vehicles [13] to deliver low cost and high assurance monitoring strategies.

To test the model predictions, as well as current and evolving technologies and techniques for detecting, attributing and quantifying leakage, a sub-seafloor CO_2 leak was simulated at a proposed CCS site.

2. Methods and logistics

2.1. Site selection

The chosen experimental site was above the Goldeneye hydrocarbon complex in the North Sea, located approximately 100 km north-east of Aberdeen, Scotland (Fig. 1a). The Goldeneye storage complex is a proposed CCS reservoir. The water depth at the experimental release site was 120 m. The site was situated 800 m from the platform (Fig. 1b), where near-surface sediments of the Witch Ground Formation are relatively soft, comprising 2.5 m of silty sediment overlying a 0.4 m sand layer, that in turn overlies a layer of silty mud between 8 and 17 m thick [14] (Fig. 1c).

2.2. Gas supply and control

Creating a simulated CO_2 leak at the Goldeneye site was technically challenging, the sub-seabed gas outlet was achieved by inserting a rigid, pre-curved steel pipe downwards into the sediment such that it followed its own curvature to describe a U-shaped path with its leading end stopping 3 m below the sediment/water interface and 1 m above its lowest point. The outlet end being significantly higher than the lowest point was designed to prevent the gas from tracking back up the outside of the pipe/sediment interface. Horizontally, the outlet end was approximately 7 m distant from the insertion point which, allowing for the landing footprint of the insertion rig, guaranteed the seabed surface remained undisturbed for at least 5 m from the outlet. The inlet end of the pipe remained protruding approximately 0.5 m above the seabed and was equipped with a quick-connect coupling for later connection to the gas supply.

The pipe insertion rig was a bespoke machine designed and built by Cellula Robotics (Burnaby, Canada). It comprised a 2.3 m cubic steel frame housing a subsea hydraulic power pack and a set of drive rollers that clamped the outside of the pipe and drove it axially into the sediment. The 6-tonne rig was complemented with lights and live video that enabled confirmation of a suitable site prior to landing (e.g., free from rocks or debris) and monitoring progress of the insertion process. Other features included a USBL beacon for recording of precise insertion location and a compass to indicate direction of the inserted pipe.

The rig was powered electrically and hydraulically from the ship via an umbilical cable that also carried engineering data and live video. The rig remained attached to the ship's winch wire throughout the insertion process and was recovered immediately on completion.

The CO_2 gas supply was stored in liquid state in a pair of 2.8 m^3 capacity bespoke storage tanks, connected to act as one storage volume. This tank was sufficient to accommodate 3 tonnes of liquid CO_2 with a 1.7 m^3 vapour headspace at 20 °C. Cryogenic storage was not viable offshore so the tanks were uninsulated and the CO_2 was stored at ambient temperature; water temperature at the 120 m deployment depth was around 8 °C which resulted in a gas pressure of 42 bar. The two tanks were mounted in a steel deployment frame of similar size to a 20-foot ISO shipping container. The frame also housed the additional tracer gases, gas mixing and control equipment, batteries, and flexible hoses for connection to the sub-seabed release pipe. CO_2 was supplemented with precise ratios of tracer gases (58.98 ppm Kr, 1.77 ppm SF_6, 0.11 ppm C_3F_8).

The gas tank frame was deployed over the aft of the ship and lowered to the seabed 80 m distant from the release pipe (Fig. 1B) to minimise any water flow disturbance at the release site during the experiment. A flexible, non-buoyant hose was extended from the gas tank frame by the Remotely Operated Vehicle (ROV) and connected to the quick-connect coupling on the exposed release pipe inlet. The gas flow was controlled by adjusting flow controllers on the gas frame using the ROV. The release rate was increased over the course of the experiment from zero to 286 kg/d.

Sensors of various types, described below, were placed on the seabed around the expected point of gas release using the ROV. Once gas was seen bubbling out of the sediment the locations of the equipment was further refined to ensure the optimal positioning for the various approaches used for gas detection, attribution and quantification. The ROV was also used to sample water and gas above the release site and replace/relocate the sensing systems when needed (Fig. 1C). Close to the release site the ROV was used to map the distribution of the dissolved CO_2, using high sensitivity optode based pH sensors alongside off the shelf ISFET based sensors. The mapping involved precisely driving the ROV on several vertical and horizontal transects across the experimental release site.

2.3. pH eddy covariance

Eddy covariance is a technique that has been used to calculate fluxes from sediments into an overlying water column. The eddy covariance flux [15] of hydrogen ions was calculated as the product of high frequency (5 Hz) turbulent fluctuations in vertical velocity and hydrogen ion concentration. The measurement location was 16 cm above the seafloor and 2.6 m from the approximate centre of the bubble streams. Vertical velocity was determined with an acoustic Doppler velocimeter. Hydrogen ion concentration was determined with an Ion Sensitive Field Effect Transistor (ISFET) mounted in a flow-through housing [16]. A gear pump pulled water from the measuring volume of the velocimeter to the ISFET at a flow rate of 0.15 L min^{-1}. The gear pump periodically reversed flow direction to expel accumulated debris. The ISFET signal was amplified ten-fold by a custom-built, auto-zeroing amplifier with temperature compensation. An AgCl reference electrode, with ceramic membrane to reduce velocity-sensitivity, was used in conjunction with the ISFET. The 90% response time of the ISFET signal was 1.2 s. The flux of hydrogen ions was calculated in half-hour intervals according to standard eddy covariance procedures [17]. The dissolved inorganic carbon flux was calculated from hydrogen ion flux using the known equilibrium change in seawater pH caused by a known addition of CO_2 [18]. For those calculations, the carbonate system was characterized by lab-on-chip measurements of pH [19,20] and alkalinity made immediately beside the eddy covariance sensors during the experiment.

2.4. Chemical gradient measurements for CO_2 flux measurements

Lab-on-chip sensors were mounted on landers and measured the pH and alkalinity at approximately 2.6 m south of the plume [20]. Each sensor had two intakes, at two heights above the seafloor (17 cm, 87 cm), and alternated measurements between these to characterize the time-dependent vertical gradient of each parameter. The current magnitude and direction were each measured at two heights: at 16 cm, with the current meter on the eddy covariance system on the same lander, and at 1.2 m with a current meter on the on another lander, 375 m away.

The total excess dissolved organic carbon (δDIC) contained within the plume was estimated from this data by taking advantage of the fact that the ellipsoidal currents caused the entire plume to sweep over the sensors once per tidal cycle. By summing the δDIC(t) over a tidal cycle we estimated the total δDIC of the plume during that cycle. To achieve this, pH and alkalinity data from the sensors were converted to DIC using the CO2SYS software [21,22] (using the time-averaged alkalinity value of TA = 2311 μmol/kg and with nutrient concentrations, temperature T

Table 1
Summary of CO_2 injection flow rates at 120 m water depth and associated volumes and masses.

		CO_2 injection		
Start (date time UTC)	End (date time UTC)	Normal L/min	g/min	kg/d
May 11, 2019 15:19	May 14, 2019 15:27	2	4	6
May 14, 2019 15:27	May 15, 2019 06:48	5	10	14
May 15, 2019 06:48	May 17, 2019 16:54	10	20	29
May 17, 2019 16:54	May 19, 2019 15:50	30	59	86
May 19, 2019 15:50	May 22, 2019 11:17	50	99	143

= 7.74 °C, and salinity S = 35.25 as measured in the area). The two points of δDIC(t) at the lander were used to parameterize a full vertical δDIC(z,t) distribution based on a model of the bubble dissolution at the source. The vertical current profile u(z,t) was estimated with the current measurements and a log-law velocity profile.

The total mass flow rate Q of the CO_2 into the water column at each point in time was estimated by

$$Q(t) = \int_{seafloor}^{openwater} \delta DIC(z,t) * u(z,t) * w(t) dz$$

where w(t) the physical east-west width of the plume that each measurement represents, z water depth. w(t) was estimated by combining the duration of the measurements with the setup geometry and time-varying current direction. To estimate the total content of the plume, the values of Q(t) for each complete current cycle were summed.

2.5. Impacts of CO_2 release on sediment porewater chemistry

The release of CO_2 into sediments can alter the chemistry of porewaters in sediments and these changes could potentially be used as indicators of leaking CO_2 from storage sites. To assess this we deployed an autonomous deep sea microprofiler, to look at chemical changes in the upper 10 cm of the sediments. Microprofiles were measured in the sediments along 4–20 m long transects from the outside of the area towards the vent area. The in situ deep-sea microsensor profiler [23] was equipped with microsensors [24] for O_2, H_2S, pH, ORP (oxidation-reduction potential) and temperature. In addition the ROV took core samples up to 30cm in length which were analysed for redox sensitive elements such as iron and manganese.

2.6. Acoustics

To determine if it was possible to image gas in the sediments above the release site we used a high resolution seismic reflection data collected using a chirp profiler (14–21 kHz) integrated on a GAVIA Autonomous Underwater Vehicle (AUV) system. The AUV-chirp data was collected at either 2 or 7.5 m elevations above the seabed, with a line separation of 2–5 m. The data has a vertical resolution of 2 cm and a horizontal resolution at a depth of 3 m (i.e. the release point) of 70 cm–100 cm.

To demonstrate the use of acoustic system for the flux of the gas from the sediments an array of 5 calibrated hydrophones was deployed 3.3 m (Fig. 1) away from the locus of injection to record the acoustic signature of gaseous CO2 bubbles emitted from the seabed into the water column and calculate CO_2 fluxes using inversion methods [25].

Further details of the experimental design and logistics can be found in Flohr et al. 2020 [26].

3. Results and discussion

During the experiment 675 kg of CO_2, with added tracers, was injected at 3 m depth into the sediment over a period of 12 days [26]. The release of CO_2 was initiated at 6 kg day^{-1} on May 11, 2019 and the flow rate was increased in a stepwise manner to a maximum flow rate of 143 kg day^{-1} (Table 1) similar to measured gas flow rates observed at leaking abandoned wells [27].

3.1. Detection

Aside from designing cost-efficient search strategies, the key element for successful leakage detection are sensors that can be deployed remotely and detect potentially small anomalies from a distance with high fidelity. Active acoustics were highly effective at detecting CO_2 bubbles in the water column and CO_2 gas accumulation in sediments. Within minutes of the start of injection at the lowest rate, bubbles were observed in the backscatter of the hull mounted (EK60) shipboard acoustic system. In 120 m water depth the shipboard system had a seabed swath of 15 m and was able to detect bubble streams with a spatial footprint of only a few metres. The fast dissolution of the CO_2, along with tidally modulated reduction in bubble flow due to changing head pressure, may limit this form of detection [28]. This approach is unable to identify the gas species that are in the bubbles. Close to the

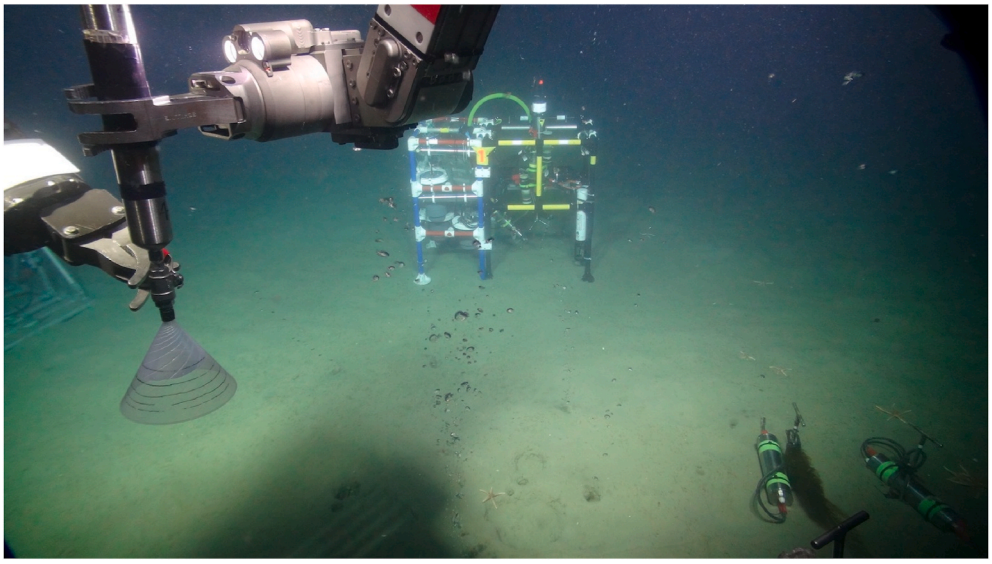

Fig. 2. Photograph of a vertical stream of gas bubbles emitted from seafloor. The left manipulator arm of the remotely operated vehicle closing the inlet valve of the gas bubble sampler in the left foreground, a lander with autonomous geochemical sensors in the centre back, and the right shows optode sensors in the sediment.

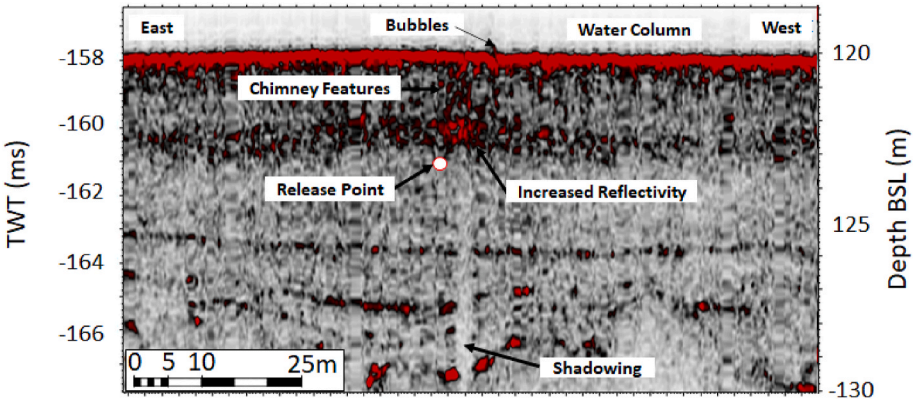

Fig. 3. Chirp sub-bottom profile over the controlled CO_2 release site (white dot) when the release rate was 143 kg day^{-1} and 361 kg had been injected. The enhanced reflectivity from 3.0 to 2.5 m beneath the seabed shows the pooling of gas within a sandier unit. There is inflation of reflectors due to the presence of gas, and the generation of vertically aligned reflectivity which are interpreted as fluid flow conduits to the seabed (chimneys). The chirp profiler data was collected from an autonomous underwater vehicle at an elevation of 2 m. The profile position is shown in Fig. 1.

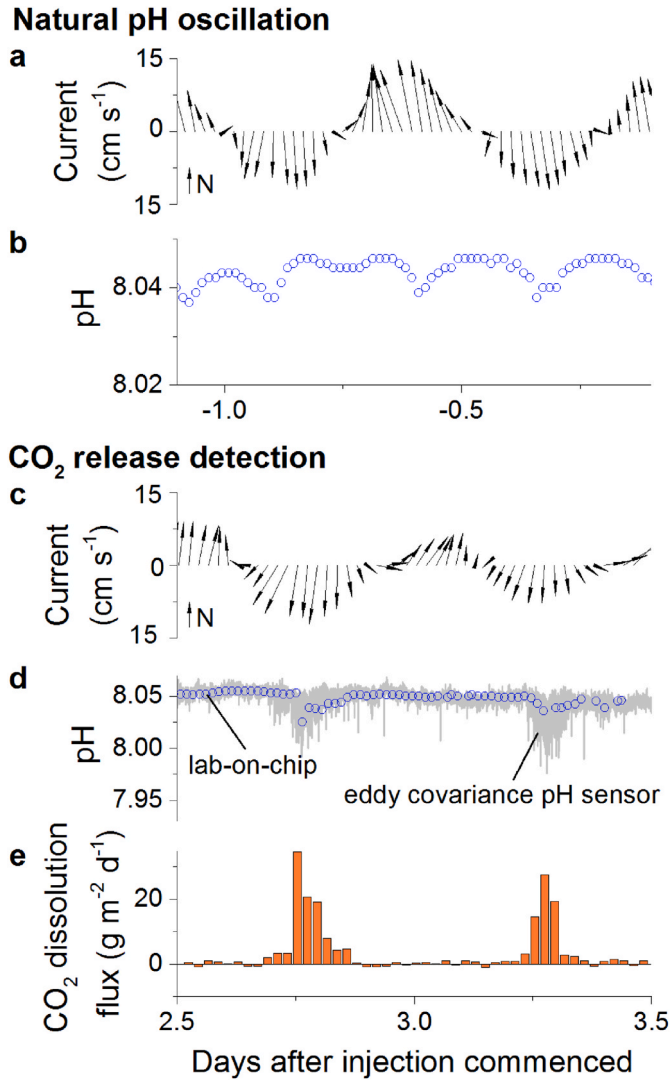

Fig. 4. Natural, leak-like pH variation before release commenced and detection of CO_2 emission using aquatic eddy covariance (injection rate 6 kg day^{-1}). **a**, **b** Natural baseline oscillations in pH due to the effect of tidal currents on thermal stratification (measured by lab-on-chip pH sensor). **c, d** After injection commenced, the low pH signal from CO_2 bubble dissolution was observed on south-bound flow (note change in pH scale). **e**, Detection of CO_2 emission by pH eddy covariance. A small, net positive flux was observed during north-bound flow (one-tailed *t*-test, $p < 0.05$) due to naturally occurring CO_2 production in sediments.

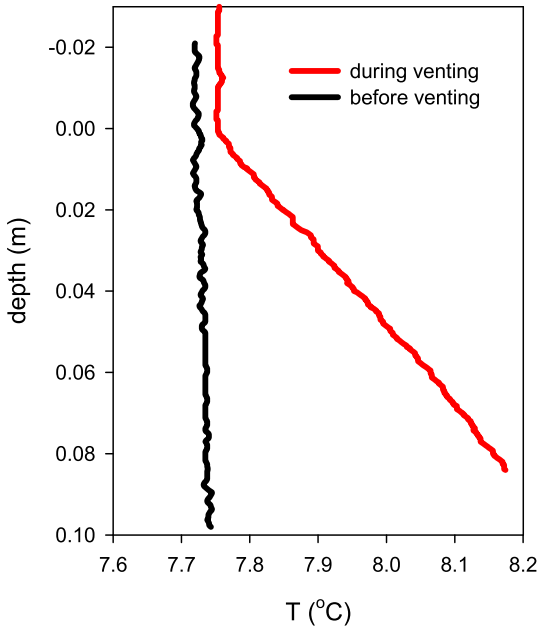

Fig. 5. Thermal changes in sediments due to carbonate and silicate mineral dissolution facilitated by released CO_2 in sediment pore waters.

leak, bubbles were seen as they emerged into the water column (Fig. 2). However, this technique relied on the use of an insitu imaging system mounted on an ROV or AUV, or a platform-based video/camera system (lander or ship deployed) and was therefore not suitable for long term autonomous monitoring.

The Chirp profiler data (Fig. 3) demonstrated increased reflectivity at 3 m depth in the seabed sediments, suggesting that gas pooled within the sandy layer, with fluid flow conduits (chimneys) visible when gas release was at a maximum. Initially gas migrated through the subsurface as individual bubbles rising upwards due to buoyancy forces (stable fracture propagation), however at higher injection rates these bubbles began to collide forming elongated fractures that rose rapidly to the surface (dynamic fracture propagation) forming open fluid flow conduits [29].

Geochemical techniques were also effective at detecting CO_2 at the lowest rates of release. Accurate and precise (better than 0.01 pH) spectrophotometric pH lab-on-chip sensors [30] detected the CO_2 leakage, 2.6 m horizontally away and 7–9 m above the leak point. This approach compensated for natural tidal mixing producing signals similar to leakage, supporting model predictions that anomalies of 0.01–0.02 ΔpH over sub-hourly timescales can be effective discriminators [10]. Further, at the lowest CO_2 injection rate, a pH eddy covariance

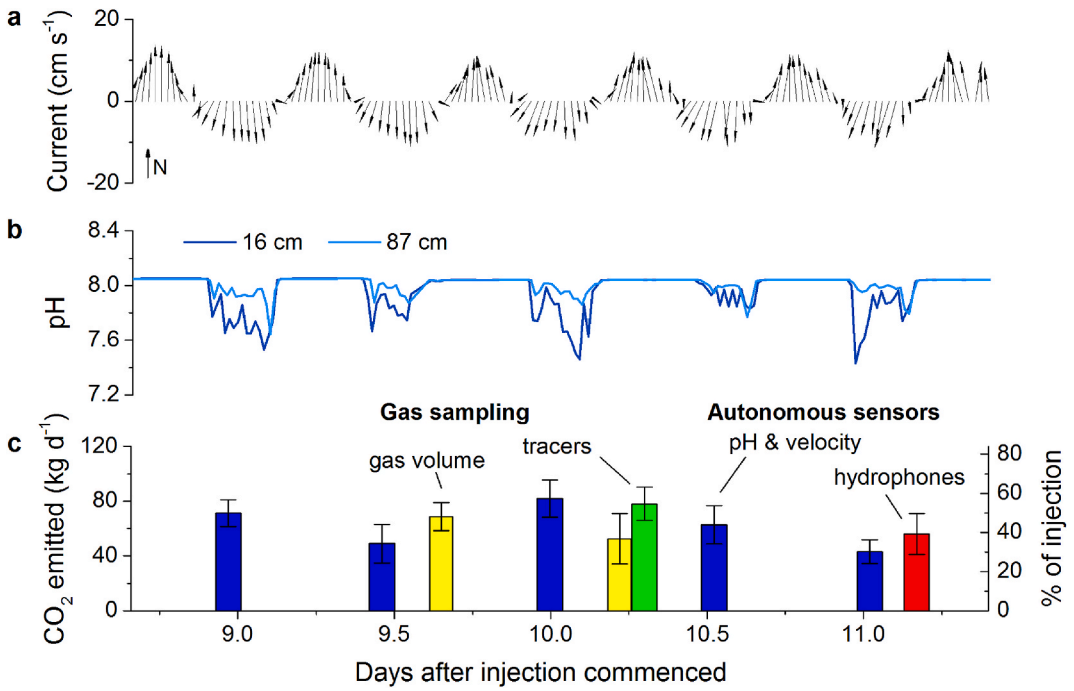

Fig. 6. Detection and quantification of total CO_2 emitted from the seafloor at the highest release rate. a, Direction and magnitude of tidal currents, which drive the CO_2-enriched water towards the chemical sensors during south-bound flow. **b**, pH of the water at 16 and 87 cm above the sea floor, 2.6 m south of the release point. **c**, estimates of the total flow rate of CO_2 emitted from the seafloor in kg day^{-1} (left y-axis) and as a fraction of actual CO_2 injection (right y-axis). These estimates are determined from: physical measurement of bubble flow rate using funnels of the gas bubble samplers ("gas volume"); analysis of tracer concentration in gaseous samples collected ~15 cm above the sea floor ("tracers"); passive acoustics measuring sound of bubble ebullition ("hydrophones"); and lab-on-chip pH measurements coupled with velocity data and models of bubble dissolution and hydrodynamics ("pH & velocity"). The first three techniques estimate gaseous CO_2 emission from seafloor while the last one estimates the total CO_2 in the plume after complete dissolution.

system (co-located 2.6 m from the centre of the bubble streams) detected significantly increased vertical fluxes in hydrogen ions, produced by CO_2(g) dissolution near the seafloor (Fig. 4). The eddy covariance technique was highly sensitive and specific: even at the lowest release rate (6 kg day^{-1}), the peak signal was 20x that of natural background CO_2 production [31].

Sediment temperature sensors were also effective for leak detection. Dissolution of CO_2 gas in sediments reduces pore water pH, triggering the dissolution of carbonate and silicate minerals. The dissolution reactions of CO_2 and carbonate minerals in pore water are exothermic, resulting in conduction of heat to the sediment surface (with a thermal gradient in excess of 5 °C m^{-1} (Fig. 5; [32]).

3.2. Attribution

To determine if a detected leak signal is naturally occurring or CCS-related, a thorough characterisation of natural geochemical conditions is needed [33]. A robust approach to attribution is to examine the stoichiometry of biologically active chemical species at the location of the signal, compared to that predicted from model or systematic observations [11,34]. For example, signals caused by natural organic matter mineralization, e.g., related to a phytoplankton bloom, will decrease pH and dissolved oxygen, whilst increasing nutrient concentrations. We confirmed this approach using novel spectrophotometric lab-on-chip pH, alkalinity, nitrate, and phosphate sensors [35,36]. Data revealed a change in pH with no equivalent change in nutrient concentrations, ruling out organic carbon remineralisation as a source of the increased CO_2 concentrations and concomitant pH drop.

The geochemical changes in the water column from the leakage in the marine system were determined by using water column sensors for pH, nitrate, alkalinity, phosphate, oxygen, H_2S and temperature. This was done by using both fine scale surveys using the ROV and wider scale surveys using an AUV equipped with pH sensors and a towed video guided CTD with pH, pCO_2 and methane sensors. The sensors indicated that changes in pH were vertically and horizontally limited to within a few metres of the bubble seep, confirming a rapid dissolution of the CO_2 bubbles that escaped across the seabed [37].

Another option for preventing false positives is to 'label' the CO_2 in the storage reservoir with tracers: these are chemical constituents that are either inherent to the injected CO_2, arising from natural processes within the reservoir, or have been purposely added to the injected CO_2. In the release experiment natural tracers ($\delta^{13}C_{CO2}$, $\delta^{18}O_{CO2}$, CH_4) and a set of added tracer gases (octafluoropropane (C_3F_8), sulfur hexafluoride (SF_6) and krypton (Kr)) were tested for the first time in combination in a marine setting. Dissolution of injected CO_2 ($\delta^{13}C_{CO2} = +19.4 \pm 0.92$‰ VPDB) into sediment pore waters and the water column was detected by enriched stable isotopic signatures of dissolved inorganic carbon ($\delta^{13}C_{DIC}$) in pore waters (5–25‰ VPDB compared to background values of −1.9 to −4.0‰ VPDB) and in the water column (+5.22‰ VPDB compared to background values of 0.61 ± 0.03‰ VPDB) as well as by the added tracers. The gas bubbles emerging from the seafloor were analysed on board the ship for CO_2, CH_4, SF_6 and C_3F_8. This confirmed that the CO_2 collected was that which had been injected into the sediments and provided a tool for quantifying the extent of CO_2 dissolution within the sediment pore waters.

We investigated the impact that the CO_2 release had in the surface sediments above the release site, by direct in situ microsensor measurements of pH, redox potential, O_2 and temperature [38]. The venting induced highly variable and dynamic effects on the pore water profiles of O_2, pH, and redox potential, confined within the venting channel. Irregular gas bubble migration in the surface sediments induced mixing of the porewater in close proximity to the bubble release sites and hindered our ability to model porewater profiles satisfactorily [39]. The pH values occasionally dropped to below 6, because CO_2 dissolution induces carbonate and silicate mineral dissolution. The loss of CO_2 in the sediment is primarily controlled by the lateral diffusion of dissolved CO_2

Table 2
Summary of leakage rates determined by independent methods at an injection flow rate of 143 kg day^{-1} (* statistically significant outlier, weighted mean (Maximum likelihood) flux is calculated without the outlier data point). The p-value analysis tests whether data points share a common mean, by comparing each data point with the weighted mean of all the other points.

Day	Leakage into water column (kg/d)	p-value	Method
9	71 ± 10	0.3097	Gradient flux
9.5	49 ± 14	0.3312	Gradient flux
10	82 ± 14	0.1265	Gradient flux
10.5	63 ± 14	0.9626	Gradient flux
11	43 ± 9	0.0129*	Gradient flux
9.65	69 ± 10	0.4838	Funnel
10.26	52 ± 19	0.5955	Funnel
10.26	78 ± 12	0.1613	Tracer
11.17	56 ± 15	0.6785	Acoustic
Weighted Mean flux	67 ± 4.5		

away from the vent channel, explaining the observed CO_2 loss by the added tracers. Whereas natural vents are often detected using redox potential anomalies [40], artificial CO_2 leakage does not induce redox effects.

3.3. Quantification

At the peak release rate (143 kg day^{-1}), CO_2 emission into the water column were quantified by gas sampling and in situ measurements using autonomous sensors as well as acoustic techniques (Fig. 6; Table 2). With gas sampling, we quantified emission using the volume collected in an inverted funnel over time. The gas samples were also analysed for tracer content; as the added tracers are much less soluble than CO_2, the change in tracer:CO_2 ratio was used to determine the proportion of the injected CO_2 that dissolved in the sediment pore waters.

The pH reduction was greatest near the seafloor where CO_2 concentration in the water column was at a maximum (gradient flux method): 2.6 m downstream of the bubble streams, the sensors recorded negative pH anomalies (0.3–0.5 pH) 16 cm above the seafloor, and 0.1–0.2 pH units at 88 cm altitude (Fig. 6b). The total mass of CO_2 emitted into the water column calculated from pH measurements in combination with water velocities and direction to determine the spatial coverage of the plume and its rate of transport was between 43 and 82 kg day^{-1} (Fig. 6c; Table 2). In addition, autonomous hydrophones were also used to quantify gaseous CO_2 emergence from the sediment from the "plop" sound made as surface tension encloses a bubble [41] (56 ± 15 kg day^{-1}; Fig. 6c). Based on these autonomous sensors, 30%–57% of the injected CO_2 gas was emitted into the water column, a greater proportion than that observed during a previous experiment in shallow waters off the west coast of Scotland [28]. All of these rates of emission agree with rates determined directly by gas sampling. Therefore, autonomous techniques are capable of quantifying CO_2(g) emission even at relatively low rates consistent with gas leakage along the outside of abandoned wells [42].

Analysis of the CO_2 in the water column (Table 2), indicates that 53% ± 3% of the injected CO_2 remained within the sediments in gaseous and dissolved form, equivalent to 360 ± 20 kg of CO_2 over the duration of the experiment (11 days). Approximately 91 ± 32 kg of gas was detected in sediments by the Chirp sub-bottom profiler after 361 kg had been injected, meaning 25% ± 9% of the injected gas remained in the sediment in gaseous form [29]. The remainder (22% ± 12%) was presumed to be dissolved in the sediment pore water by this point in the experiment; eventually all gaseous CO_2 will go into solution and be neutralized by reaction with carbonate and silicate minerals. As discussed above, elevated temperature and reduced pH in sediment porewaters measured using microprofilers evidence CO_2 dissolution. Fracture-generated, stable open conduits between the release point and the seabed [29] nevertheless limit the extent of CO_2 dissolution in sediments, permitting near-instantaneous flow of gaseous CO_2.

From Table 2 it can be noted that with the exception of one result obtained from the Gradient flux method, 8 of the 9 measurements are not statistically different from each other ($p > 0.05$) and yield a flow rate of 67 ± 4.5 kg day^{-1}, which is remarkably consistent considering the complexity of the marine environment and the different approaches taken.

At Goldeneye, the naturally occurring annual pH range in bottom waters is 0.15 pH units [43]. CO_2 driven impacts on biogeochemical processes are generally not seen with perturbations less than 0.1 pH units below the natural range [44]. The volume of water in which the reduction of pH was greater than 0.15 units was estimated from experimental data to be 17 m^3 downstream of the site, based on the ROV's pH spatial surveys. This was very consistent with pre-experiment models which estimated that this volume would be 21 m^3, similarly the volume acidified by≥0.01 pH unit is calculated as 1000 m^3, which validate model-derived estimates which predict 815 m^3 for the same release rate [45]. This demonstrates that the volume of water affected by a readily detected leak is quite small [46] and validates the use of models in predicting this volume, but also illustrates the challenge in monitoring an affected volume of such small size. In the sediments, pH reduction of >0.15 units in the very surface sediments (uppermost 10 cm) was limited to a radius of a few centimeters, indicating that the CO_2 rose vertically and entered the water column. The experimental release had a short duration, but our results approximate steady state conditions due to the effectiveness of seawater buffering of pH and rapid mixing.

4. Conclusions

To make CO_2 storage in terrestrial geological reservoirs an effective and safe long-term CO_2 removal strategy, acceptable surface leakage rates (i.e. CO_2 escaping back into the atmosphere) of 0.01% reservoir loss per year have been proposed [47]. No such acceptable leakage rates have been proposed for the marine environment. Applying the above terrestrial leakage rates to the injection of 1 Mt/yr over 20 years that was projected for the Goldeneye reservoir [48], corresponds to acceptable leakage rates of 274 kg/d after the first year of injection and 5480 kg/d after 20 years of injection when full storage capacity is reached. During the STEMM-CCS release experiment CO_2 gas was injected at flow rates of up to 143 kg/d and leakage into the water column ranged between 43 and 82 kg/d. The injected CO_2 was detected in all its forms (gaseous and dissolved in the sediments, and gaseous and dissolved in the water column) during the experiment. As CO_2 leakage is unlikely to be continuous over the whole reservoir area but is more expected to be preferentially transported through small, focused fractures and faults or through poorly-sealed abandoned wells [6], both the flow rates and the type (point-release) of our simulated leakage suggest that for practical purposes a 0.01% loss threshold could be adopted for offshore storage.

Previous work has demonstrated that the environmental recovery from small leaks – on the order of under 1000 kg/d, is measurable in days to weeks [28]. The impacted area, but more crucially detection length scale, correlate with release rate [45], thus with the techniques demonstrated here we are confident that non-catastrophic leaks can be detected, attributed, and quantified at a lower release rate than that which causes significant environmental harm. While this paper focusses on "leakage" across the seabed, it should be noted that any approved Carbon Capture Storage Complex will have multiple barriers which make leakage extremely unlikely, with full monitoring and mitigation controls in place [49,50].

The work described herein allows us for the first time to demonstrate that we are able to detect, attribute and quantify CO_2 leakage from an

Table 3
Summary of techniques used during the experimental gas release. D, Detection; A, Attribution; Q, Quantification. Shaded cells represent methods/analyses performed in-situ, and unshaded cells represent methods that relied on sample collection and subsequent analysis on board the ship or on shore.

Measurement target	Technique/method	D	A	Q
Seafloor and sub-seafloor	Benthic biological imaging	x		
	Sediment coring	x	x	
	Sediment microprofiler	x		
	Sediment optodes	x		
	AUV Chirp Profiler	x		x
Gaseous CO_2 in the water column	Bubble imaging			x
	Funnel capture of gas bubbles			x
	Gas sampling	x	x	x
	Passive acoustics	x		x
	Multibeam and sidescan acoustics	x		
	Video-CTD imaging	x		
Dissolved CO_2 in the water column	Niskin bottle sampling	x	x	
	In situ/pumped CTD sampling	x	x	x
	Benthic chambers	x	x	x
	Eddy covariance	x	x	x
	Chemical gradient measurements	x	x	x
	Chemical mapping with ROV	x	x	
	pH sensing on an AUV	x		

offshore carbon dioxide storage reservoir. With the techniques demonstrated here (Table 3) we are confident that non-catastrophic leaks can be detected, attributed, and quantified at a far lower release rate (6 kg day^{-1}) than that which causes significant environmental harm. The work demonstrates the importance of using model-derived approaches in combination with observed data to determine what is possible using current and emerging technologies and approaches. It informs the application of legislation and allows the design of cost efficient monitoring programmes to be used by operators.

Author contributions

Conceptualization: Connelly, D.P., Bull, J.M., Achterberg, E.P., James, R.H., Blackford, J.C, Dean, M., Mowlem, M.C.

Methodology: Borisov, S.M, Flohr, A., Lichtschlag, A., Loucaides, S., Leighton, T.G., LeBas, T., Matter, J.M., Saleem, U., Schaap, A., Schramm, B., Omar, A.M., Falcon Suarez, I., Ungerboeck, B.

Engineering design: Saw, K., Brown, R., Wright, H.

Modelling: Avleson, A., Blackford, J.C., Chen, B., Dewar, M., Oleynik, A., Haeckel, M., Cazenave, P.W., Provenzano, G., Yakushev, E.

Field and experimental work: Connelly, D.P., Bull, J.M., Böttner, C., Achterberg, E.P, , Flohr, A., Hosking, B., Koopmans, D., Karstens, J., de Beer, D., White, P.R., Roche, B., Esposito, M., Dale, A.W., Gros, J., Hanz, R., Huvenne, V., Linke, P., Monk, S., Peel, K., Schaap, A., Schmidt, M., Sommer, S., Widdicombe, S., Strong, J. Li, J.

Funding acquisition: Connelly, D.P., Bull, J.M., Achterberg, E.P., James, R.H., Blackford, J.C, Dean, M., Mowlem, M.C.

Writing: Connelly, D.P., Bull, J.M., Achterberg, E.P., James, R.H., Blackford, J.C., Flohr, A., Schaap, A., Koopmans, D., deBeer, D., White, P.R., Roche, B., Lichtschlag, A., EA, RHJ, Pearce, C.

Data and materials availability

All data from the shipboard operations are available in Pangaea or the BODC data repositories.

Methane and CO_2 data, POS527: https://doi.org/10.1594/PANGAEA.910413.

ADCP data, POS534: https://doi.org/10.1594/PANGAEA.908919.

Lander ADCP data and biogeochemical data POS518 and JC180: https://doi.org/10.1594/PANGAEA.908935, https://doi.org/10.1594/PANGAEA.909624.

Physical oceanography data POS534: https://doi.org/10.1594/PANGAEA.910583.

Cruise report and cruise track.

JC180: https://www.bodc.ac.uk/resources/inventories/cruise_inventory/report/17236/

Declaration of competing interest

The authors declare that they have no known competing financial interests or personal relationships that could have appeared to influence the work reported in this paper.

Acknowledgements

Funding was provided by the European Unions Horizon 2020 research and innovation programme under the grant agreement number 654462 (STEMM-CCS). We are grateful to the Captains and crews of the RRS James Cook and RV Poseidon for enabling the scientific measurements at sea during the JC180 and POS518, POS527, POS534 and MSM63 and MSM68 cruises. Mark Wells and the team at Cellular Robotics are thanked for the development of the seabed drilling system. We thank the support team at the National Marine Facilities at the NOC in Southampton for their unstinting help in the planning of the complex cruise programme.

References

[1] Metz B, Davidson O, de Coninck HC, Loos M, Meyer LA. IPCC special report on carbon dioxide capture and storage. In: Prepared by working group III of the intergovernmental Panel on climate change. United kingdom and New York, NY, USA. Cambridge: Cambridge University Press; 2005.
[2] Ringrose PS, Meckel TA. Maturing global CO2 storage resources on offshore continental margins to achieve 2DS emissions reductions. Sci Rep 2019;9:17944.
[3] Meckel TA, Trevino R, Carr D, Nicholson A, Wallace K. Offshore CCS in the northern Gulf of Mexico and the significance of regional structural compartmentalization. Energy Proc 2013;37:4526–32.
[4] Beck L. Carbon capture and storage in the USA: the role of US innovation leadership in climate-technology commercialization. Clean Energy 2020;4:2–11.
[5] Ec. Directive 2009/31/EC of the European Parliament and the Council of 23 April 2009 on the geological storage of carbon dioxide. 2009. Amending Council Directive 85/337/EEC, European Parliament and Council Directives 2000/60/EC, 2001/80/EC, 2004/35/EC, 2006/12/EC, 2008/1/EC and Regulation (EC) No.1013/2006.
[6] Ec. Commission Regulation (EU) No. 601/2012 of June 2012 on the monitoring and reporting of greenhouse gas emissions pursuant to Directive 2003/87/EC of the European Parliament and of the Council. E. Commission. Website of the European Commission - Climate Action – EU Action - Emissions Trading System - Monitoring & Reporting; 2012.
[7] Blackford J, et al. Marine baseline and monitoring strategies for carbon dioxide capture and storage (CCS). Int J Greenh Gas Control 2015;38:221–9.
[8] Dewar M, Sellami N, Chen B. Dynamics of rising CO_2 bubble plumes in the QICS field experiment: Part 2 - Modelling. Int J Greenh Gas Control 2015;38:52–63.
[9] Gros J, et al. Simulating and quantifying multiple natural subsea CO_2 seeps at panarea island (aeolian islands, Italy) as a proxy for potential leakage from subseabed carbon storage sites. Environ Sci Technol 2019;52:10258–68.
[10] Blackford JC, Artioli Y, Clark J, de Mora L. Monitoring of offshore geological carbon storage integrity: implications of natural variability in the marine system and the assessment of anomaly detection criteria. Int J Greenh Gas Con 2017;64:99–112.
[11] Botnen HA, Omar AM, Thorseth I, Johannessen T, Alendal G. The effect of submarine CO_2 vents on seawater: implications for detection of subsea carbon sequestration leakage. Limnol Oceanogr 2015;60:402–10.
[12] Oleynik A, García-Ibáñez MI, Blaser N, Omar A, Alendal G. Optimal sensors placement for detecting CO_2 discharges from unknown locations on the seafloor. Int J Greenh Gas Con 2020;95:362–102951.
[13] Alendal G. Cost efficient environmental survey paths for detecting continuous tracer discharges. J Geophys Res: Oceans 2017;122:5458–67.
[14] Stoker MS, Long D, Fyfe JA. A revised Quaternary stratigraphy for the central North Sea. Rep Br Geol Surv 1985;17:1–43.
[15] Berg P, et al. Oxygen uptake by aquatic sediments measured with a novel non-invasive eddy-correlation technique. Mar Ecol Prog Ser 2003;261:75–83.
[16] Long MH, Charette MA, Martin WR, McCorkle DC. Oxygen metabolism and pH in coastal ecosystems: eddy covariance hydrogen ion and oxygen exchange system (ECHOES). Limnol Oceanogr Methods 2015;13:438–50.
[17] Holtappels M, et al. Effects of transient bottom water currents and oxygen concentrations on benthic exchange rates as assessed by eddy correlation measurements. J Geophys Res: Oceans 2013;118:1157–69.

[18] Lewis ER, Wallace DWR. Program developed for CO_2 system calculations: environmental system science data infrastructure for a virtual ecosystem 1998. Web. doi:10.15485/1464255.
[19] Rérolle VMC, et al. High resolution pH measurements using a lab-on-chip sensor in surface waters of Northwest. European shelf seas. Sensors 2018;18:2622.
[20] Rérolle VMC, et al. Development of a colorimetric microfluidic pH sensor for autonomous seawater measurements. Anal Chim Acta 2013;786:124–31.
[21] Lewis E, Wallace DWR. Program developed for CO2 system calculations, ORNL/CDIAC-105. Carbon Dioxide Inf. Anal. Cent., Oak Ridge Natl. Lab., Oak Ridge, Tenn.; 1998. p. 38. https://salish-sea.pnnl.gov/media/ORNL-CDIAC-105.pdf.
[22] van Heuven S, Pierrot D, Rae JWB, Lewis E, Wallace DWR. MATLAB program developed for CO_2 system calculations. Oak Ridge, Tennessee: ORNL/CDIAC-105b. Carbon Dioxide Information Analysis Center, Oak Ridge National Laboratory, U.S. Department of Energy; 2011. https://doi.org/10.3334/CDIAC/otg.CO2SYS_MATLAB_v1.1.
[23] Glud RN, et al. High rates of benthic microbial activity at 10.900 meters depth: results from the challenger deep (mariana trench). Nat Geosci 2013;6:284–8.
[24] Fink A, den Haan J, Chennu A, Uthicke S, de Beer D. Ocean acidification changes abiotic processes but not biotic processes in coral reef sediments. Front Mar Sci 2017;4:73.
[25] Leighton TG, White PR. Quantification of undersea gas leaks from carbon capture and storage facilities, from pipelines, and from methane seeps, by their acoustic emissions. Proc R Soc A 2012;468:485–510.
[26] Flohr A, et al. Towards improved monitoring of offshore carbon storage: a real-world field experiment detecting a controlled sub-seafloor CO_2 release. Int J Greenh Gas Con 2020;106:103327.
[27] Vielstädte L, et al. Quantification of methane emissions at abandoned gas wells in the Central North Sea. Mar Petrol Geol 2015;68:848–60.
[28] Blackford J, et al. Detection and impacts of leakage from sub-seafloor deep geological carbon dioxide storage. Nat Clim Change 2014;4:1011–6.
[29] Roche B, et al. Time-lapse imaging of CO2 migration within near-surface sediments during a controlled sub-seabed release experiment. Int J Greenh Gas Con 2021;109:103363.
[30] Rérolle VMC, Floquet CFA, Mowlem MC, Achterberg EP. Seawater-pH measurements for ocean-acidification observations. Trends Anal Chem 2012;40:146–57.
[31] Koopmans D, et al. Detection and quantification of a release of carbon dioxide gas from the seafloor using pH eddy covariance and measurements of plume advection. Int J Greenh Gas Con 2021;112:103476.
[32] de Beer D, et al. Sediment acidification and temperature increase in an artificial CO_2 vent. Int J Greenh Gas Con 2021;105:103244.
[33] Dixon T, Romanak KD. Improving monitoring protocols for CO2 geological storage with technical advances in CO2 attribution monitoring. Int J Greenh Gas Con 2015;41:29–40.
[34] Romanak KD, Bennett PC, Yang C, Hovorka SD. Process-based approach to CO2 leakage detection by vadose zone gas monitoring at geologic CO2 storage sites. Geophys Res Lttrs 2012;39:L15405.
[35] Beaton AD, et al. Lab-on-Chip measurement of nitrate and nitrite for in situ analysis of natural waters. Environ Sci Technol 2012;46:9548–56 (2012).
[36] Clinton-Bailey GS, et al. A Lab-on-Chip analyzer for in situ measurement of soluble reactive phosphate: improved phosphate blue assay and application fluvial monitoring. Environ Sci Technol 2017;51:17.
[37] McGinnis DF, et al. Discovery of a natural CO_2 seep in the German North Sea: implications for shallow dissolved gas and seep detection. J Geophys Res Oceans 2011;116.
[38] de Beer D, et al. Saturated CO_2 inhibits microbial processes in CO_2-vented deep-sea sediments. Biogeosciences 2013;10:5639–49.
[39] Lichtschlag A, et al. Impact of CO_2 leakage from sub-seabed carbon dioxide capture and storage on sediment geochemistry. Int J Greenh Gas Con 2021;109:103352.
[40] Konno U, et al. Liquid CO_2 venting on the seafloor: yonaguni knoll IV hydrothermal system, okinawa trough. Geophys Res Lett 2006;33:L16607.
[41] Li J, et al. Acoustic and optical determination of bubble size distributions – quantification of undersea gas emissions. Int J Greenh Gas Con 2021;109:103313.
[42] Bottner C, et al. Greenhouse gas emissions from marine decommissioned hydrocarbon wells: leakage detection, monitoring and mitigation strategies. Int J Greenh Gas Con 2020;100:103119.
[43] Esposito M, et al. Water column baseline assessment for offshore Carbon Dioxide Capture and Storage (CCS) sites: analysis of field data from the Goldeneye storage complex area. Int J Greenh Gas Con 2021;109:103344.
[44] Doney SC, Busch DS, Cooley SR, Kroeker KJ. The impacts of ocean acidification on marine ecosystems and reliant human communities. Annu Rev Environ Resour 2020;45:11.1–11.30.
[45] Blackford J, et al. Impact and detectability of hypothetical CCS offshore seep scenarios as an aid to storage assurance and risk assessment. Int J Greenh Gas Control 2020;95:102949.
[46] Vielstädte L, et al. Footprint and detectability of a well leaking CO_2 in the Central North Sea: implications from a field experiment and numerical modelling. Int J Greenh Gas Con 2019;84:190–203.
[47] Hepple RP, Benson SM. Geologic storage of carbon dioxide as a climate change mitigation strategy: performance requirements and the implications of surface seepage. Int J Environ Geol 2005;47:576–85.
[48] Dean M, Tucker O. A risk-based framework for Measurement, Monitoring and Verification (MMV) of the Goldeneye storage complex for the Peterhead CCS project, UK. Int J Greenh Gas Con 2017;61:1–15.
[49] Jenkins CR, et al. Safe storage and effective monitoring of CO_2 in depleted gas fields. Proc Natl Acad Sci Unit States Am 2012;109. E53-41.
[50] Alcalde J, et al. Estimating geological CO_2 storage security to deliver on climate mitigation. Nat Commun 2018 2018;9:2201.